Eur. Phys. J. D **14**, 217–223 (2001)

THE EUROPEAN PHYSICAL JOURNAL D

EDP Sciences

Laser excitation and ionic motion in small clusters

L.M. Ma[1], E. Suraud[1,a], and P.-G. Reinhard[2]

[1] Laboratoire de Physique Quantique, Université Paul Sabatier, 118 route de Narbonne, 31062 Toulouse Cedex, France
[2] Institut für Theoretische Physik, Universität Erlangen, Staudstrasse 7, 91054 Erlangen, Germany

Received 13 October 2000 and Received in final form 18 December 2000

Abstract. We discuss the properties of small metal and hydrogen clusters under irradiation by intense lasers. We use a fully non adiabatic model of coupled electrons and ions, based on density functional theory. We demonstrate the quality of such an approach in comparison to experimental data on atomic and molecular properties as well as to the optical response of small sodium clusters. We next address the response of small clusters to various lasers allowing to scan a broad span of dynamical regimes from the linear to the non linear domain. We finally discuss the impact of ionic motion in the case of hydrogen clusters irradiated by short laser pulses in the $10^{13}-10^{15}$ W cm^{-2} intensity range.

PACS. 36.40.-c Atomic and molecular clusters – 36.40.Cg Electronic and magnetic properties of clusters – 36.40.Vz Optical properties of clusters

1 Introduction

The excitation of molecules and clusters with fs laser pulses is an extremely versatile tool to trigger and to analyse a world of dynamical processes. These processes range from the simple optical response [1] to multi-photon ionisation [2] and/or the various scenarios of Coulomb explosion of clusters [3,4]. An appropriate theoretical description requires a fully-fledged coupled ionic and electronic dynamics because the violent excitations by fs lasers quickly drive the system beyond the Born-Oppenheimer surface. At the side of the electronic dynamics, one has at hand the manageable and well tested time dependent Density Functional Theory at the level of the time-dependent local-density approximation (TDLDA) [5]. The ions can usually be treated by classical molecular dynamics (MD). An appropriate tool for describing the fs laser excitations thus turns out to be a coupled TDLDA-MD, for a review see [6]. There exist already a few studies of dynamical scenarios using TDLDA-MD, *e.g.* to understand the experimental findings of [4] with a simulation of Coulomb expansion and subsequent plasmon-enhanced laser attenuation for medium size Na clusters [7] or to scan the sensitivity of explosion dynamics on the laser parameters [8]. But up to now, most of these elaborate fully dynamical calculations have been restricted (particularly in the non-linear domain) to simple metal clusters such as sodium clusters [6]. There is a world of other materials to be attacked with TDLDA-MD. One particularly interesting case are hydrogen clusters, first, because hydrogen is a generic material whose metallic or non-metallic behaviour has raised much attention recently [9], and second because Coulomb explosion of hydrogen clusters seems to be an extremely interesting process [3]. The heavy isotope of hydrogen, deuterium, has recently attracted much attention due to the observation of nuclear fusion triggered by table top lasers [10]. It is one of the aims of this contribution to present a first exploration of the dynamics of small hydrogen clusters using TDLDA-MD. To put the results into perspective, analogous cases are also considered for the simple metals Na and Cs.

[a] e-mail: suraud@irsamc2.ups-tlse.fr

2 Framework

Time-dependent density-functional theory is still in a developing stage and many of the much refined approaches are yet too involved to be applicable in large scale calculations [5]. We thus refer to a robust and most efficient scheme for our description of coupled electronic and ionic dynamics, namely TDLDA for the electrons coupled to classical MD for the ions. For the TDLDA we employ the exchange-correlation functional of [11]. In the LDA, details of electron emission are spoiled by the self-interaction error, particularly for small systems. We cure that by invoking a self-interaction correction (SIC) according to the recipe of [14].

The interaction between ions and electrons is described by means of a local pseudo-potential which consists out of a sum of two error functions

$$V_{\rm psp} = -\frac{Ze^2}{r}\left\{c_1 {\rm erf}\left(\frac{r}{\sqrt{2}\sigma_1}\right) + c_2 {\rm erf}\left(\frac{r}{\sqrt{2}\sigma_2}\right)\right\}. \quad (1)$$

This form is particularly robust for numerical purposes. And the parameters can be adjusted to provide a good

Table 1. The parameters of the pseudo-potential equation (1) for the three materials under consideration. The values for Na are taken from [12], for Cs from [13], and those for H have been adjusted to reproduce the spectrum of the H atom.

	H	Na	Cs
c_1	1.809	−2.291	−0.8530
c_2	−0.8094	3.291	1.8530
$\sigma_1[a_0]$	0.2548	0.6809	0.9512
$\sigma_2[a_0]$	0.3822	1.163	2.1675

description of structure as well as of dynamics [12]. We use here the parameters as given in Table 1. The parameters for Na and Cs have been tuned to atomic spectra and bulk properties (equilibrium density, cohesive energy). They also provide reliable electronic excitation energies, particularly for plasmon resonances of clusters [12] and reasonable molecular properties as we will see below. One may wonder why we employ a pseudopotential for hydrogen where the correct potential e^2/r is well known. The reason is that the pure Coulomb potential does not comply well with a description of the wavefunctions on a spatial grid. Some smoothing of the pole at $r = 0$ is needed. A simple cutoff at small r underestimates binding of the $1s$ state. The pseudopotential allows to readjust the spectrum correctly by carefully counterweighting the smoothing at smallest r. We have constructed here a pseudopotential with rather large folding radii, because the smallest grid spacing has to be proportional to the smaller of the two widths ($\Delta = \sigma_1\sqrt{2\log 2}$). We can thus work here with a grid spacing of $\Delta = 0.3a_0$ which yields an extremely efficient numerical handling. Note that the pseudopotential converges rapidly to the correct asymptotic behaviour e^2/r such that relevant static and dynamical properties remain almost unaffected.

Ions are treated as classical particles and propagated under their mutual (point-like) Coulomb interactions together with the electron-ion forces as derived from the pseudo potential. The laser field, acting both on electrons and ions, reads $V_{\rm las} = E_0\hat{z}f_{\rm las}(t)\cos(\omega t)$ ($\hat{z}$ being the local dipole operator and $E_0 \propto \sqrt{I}$, I being the intensity). The pulse profile $f_{\rm las}(t)$ is chosen as a cosine^2 in time. The TDLDA equations are then solved numerically on a grid in 3D coordinate space. The ground state wavefunction is determined by an accelerated gradient step [15]. The time-dependent Kohn-Sham equation for electrons is solved with the time-splitting technique and a Verlet algorithm is used for the simultaneous ionic propagation. We employ absorbing boundary conditions to treat ionisation correctly. Details of this treatment can be found in the recent review [6]. We want to point out that this coupled ionic and electronic dynamics, constitutes a true TDLDA-MD, and goes beyond the usual Born-Oppenheimer molecular dynamics. This is precisely what is needed to cope with the violent off-equilibrium dynamics as induced by strong laser pulses. Indeed the pulse lifts the electronic state far off the Born-Oppenheimer surface. The state remains far from an ion-electron equilibrium for a long time and it was shown that this situation cannot be mapped into a Born-Oppenheimer dynamics [16]. In turn, this non Born-Oppenheimer dynamics is correctly described in TDLDA-MD by explicitly propagating electrons and ions in time.

Table 2. Ionisation potentials (IP) for the H, Na, and Cs atom (in units of [eV]).

	H	Na	Cs
IP exp. [eV]	13.6	5.10	3.89
IP th. [eV]	13.0	5.18	3.90
% error	4.1	1.6	0.3

Before attacking dynamical situations we shall first briefly demonstrate the capabilities of our approach to describe clusters at equilibrium. Amongst the ground state observables, we concentrate here on the ionisation potential (IP) of the atom and dimer. We compute the IP from the energy of the last occupied electron state. The SIC restores Koopmans theorem to a large degree such that this single-electron energy is almost identical to the difference of the binding energies of initial and final system. It is crucial for dynamical calculations of ionisation that the single electron states carry the correct IP. As a further ground state observable we also compute the bond length and vibration period of dimers and compare them to experimental data. For the more dynamical observables we consider predominantly the electronic dipole momenta, *i.e.* the expectation values of x, y, and z computed in a vicinity of the cluster. We look at their time dependence as such. And we deduce excitation spectra by Fourier transformation into the frequency domain which has become meanwhile a standard technique to evaluate spectra *via* TDLDA [17–19]. Ionisation is also computed as a function of time, by recording the number of electrons lost through the absorbing boundaries.

3 Results and discussion

3.1 Structure and optical response

We first check our approach for atoms. Table 2 shows the ionisation potentials (IP) for neutral atoms. The IP for neutral atoms are, of course, well reproduced because this was a data used in the construction of the pseudopotentials. (Even better values may be obtained with a smaller mesh size, at the price of more computational expense.)

The second step on the long road towards clusters and bulk material is the dimer. Table 3 summarises our results on these systems. The bond lengths are reproduced very nicely for the three materials considered here (H, Na, Cs). The curvature of the inter-atomic potential is, in turn, probed by the molecular vibration frequency. The results on that observable are also very convincing. Both features hint that the pseudo-potentials used here have the required property of transferability. The IP's of the

Table 3. Ionisation potentials, equilibrium distance d, and ionic vibration period for the H_2, Na_2, and Cs_2 dimers. The experimental data come from [26].

	H_2	Na_2	Cs_2
IP exp. [eV]	15.4	4.90	3.70
IP th. [eV]	15.9	4.93	3.55
% error	3.5	0.8	3.5
Distance exp. [a_0]	1.46	5.82	8.46
Distance th. [a_0]	1.40	5.71	8.2
% error	4.3	1.9	3.1
Period exp. [fs]	7.6	209	793
Period th. [fs]	7.3	202	777
% error	4.1	2.0	3.3

Table 4. Theoretical ionisation potentials, bond length b, and electronic excitation energies for the H_3^+, Na_3^+, and Cs_3^+ trimers obtained with LDA-SIC. Values in parenthesis for Na_3^+ are experimental data.

	H_3^+	Na_3^+	Cs_3^+
IP [eV]	31.9	9.41	6.67
bond length [a_0]	1.732	6.446	9.227
Peak in $x-y$-direction [eV]	18	2.75 (2.65)	1.6
Peak in z-direction [eV]	20.8	3.38 (3.32)	2.0

dimers fit also very well. The somewhat large error for H_2 is excused by the fact that we used a slightly too small grid. This result, in turn, indicates that hydrogen systems are more demanding numerically. But for reasons of efficiency, we carry on with these somewhat itching grids for hydrogen. The emerging uncertainty is acceptable for exploratory purposes of energetic dynamics.

Next, we proceed to the smallest cluster, the trimer. We are considering the positively charged trimers because these are more easily accessible experimentally. The three ions arrange in a regular triangle and one needs to optimise only the base length. The resulting structures and electronic densities are visualised in Figure 1. One sees a marked difference in profiles between the metallic clusters Na_3^+ as well as Cs_3^+ and the covalent H_3^+. There is more electronic density gathering near the ionic centers for H_3^+ while the electron cloud is a common property of all ions for the metal clusters. The ions induce only a moderate perturbation in Na_3^+ and even less in Cs_3^+ which has the largest diameter in our samples.

Table 4 provides more detailed (quantitative) results for the trimers. It is instructive to compare the bond lengths with the Wigner-Seitz radii of the corresponding bulk material, $r_s = 2, 4$, and $5.6a_0$ for H, Na, and Cs respectively. The ratio of the bond lengths between Cs and Na is very close to the ratio of the r_s. But the ratio of the bond length between H and Na is 1/4 whereas the ratio of the r_s is 1/2. This hints that the binding properties are different. It confirms the finding from Figure 1, namely that Na and Cs are clearly metallic systems throughout while hydrogen prefers covalent binding in its ground state. Quantum chemical calculations for Na_3^+ [20] do also find the triangular ground state configuration and the bond length is $6.41a_0$ which compares very well with our result.

The structures can be identified indirectly through their optical response. Results are given in Table 4. These simple two-electron systems have only very few excitations in the optical range. We can identify one dominant mode for excitation along x- and y-directions (these two are degenerate) and one along the z-direction. The system is more extended in the x–y-plane (see the cluster's orientations in Fig. 1). This leads to the lower excitation frequencies in this plane. The extension in the z-direction is smaller and we obtain the larger frequencies. Experimental data are available for the optical response of Na_3^+ clusters at 100 K temperature. The lower peak is found at 2.65 eV and the higher at 3.32 eV. This agrees fairly well with our results. Note that we have computed the trimer at temperature zero. A slight thermal expansion at 100 K will yield a slight red shift of the spectra which helps to improve the agreement [21].

3.2 Laser excitation

3.2.1 Linear domain

We now turn to detailed studies of time-evolution in the presence of an external (possibly intense) laser field. Figure 2 shows the electron response in the time domain for low intensity excitations staying well inside the linear regime. We have chosen the laser frequency in each case close to the lower mode, the mode in the x–y-direction, see Table 4. The laser polarisation is along the diagonal thus having equal components in x-, y-, and z-directions. We thus probe with one calculation resonant (for the x–y-mode) and off-resonant (for the z-mode) excitations. The results in Figure 2 clearly show the different responses. First, the off-resonant case (upper panels) is responding much more reluctantly as can be seen from the much smaller amplitude. Second, its envelope follows closely the laser amplitude and the signal basically disappears when the laser is switched off. This behaviour is already well known from basic mechanics in connection with the response of a simple driven harmonic oscillator. The resonant case (lower panels) behaves much differently. The onset still follows the laser amplitude. But soon the signal develops a live of its own and it continues to oscillate long after the laser has died out. The overall amplitude is, of course, much larger. We have here one more example of field amplification through resonant response [23]. The same pattern are found for Na_3^+ and also for any larger cluster [24]. We see here a feature which is generic in the linear domain.

A more detailed look at Figure 2 reveals subtle differences between H and Cs. Note the much smaller amplitude for H_3^+ which emerges although the laser intensity was much larger than the one used for Cs_3^+. This reflects

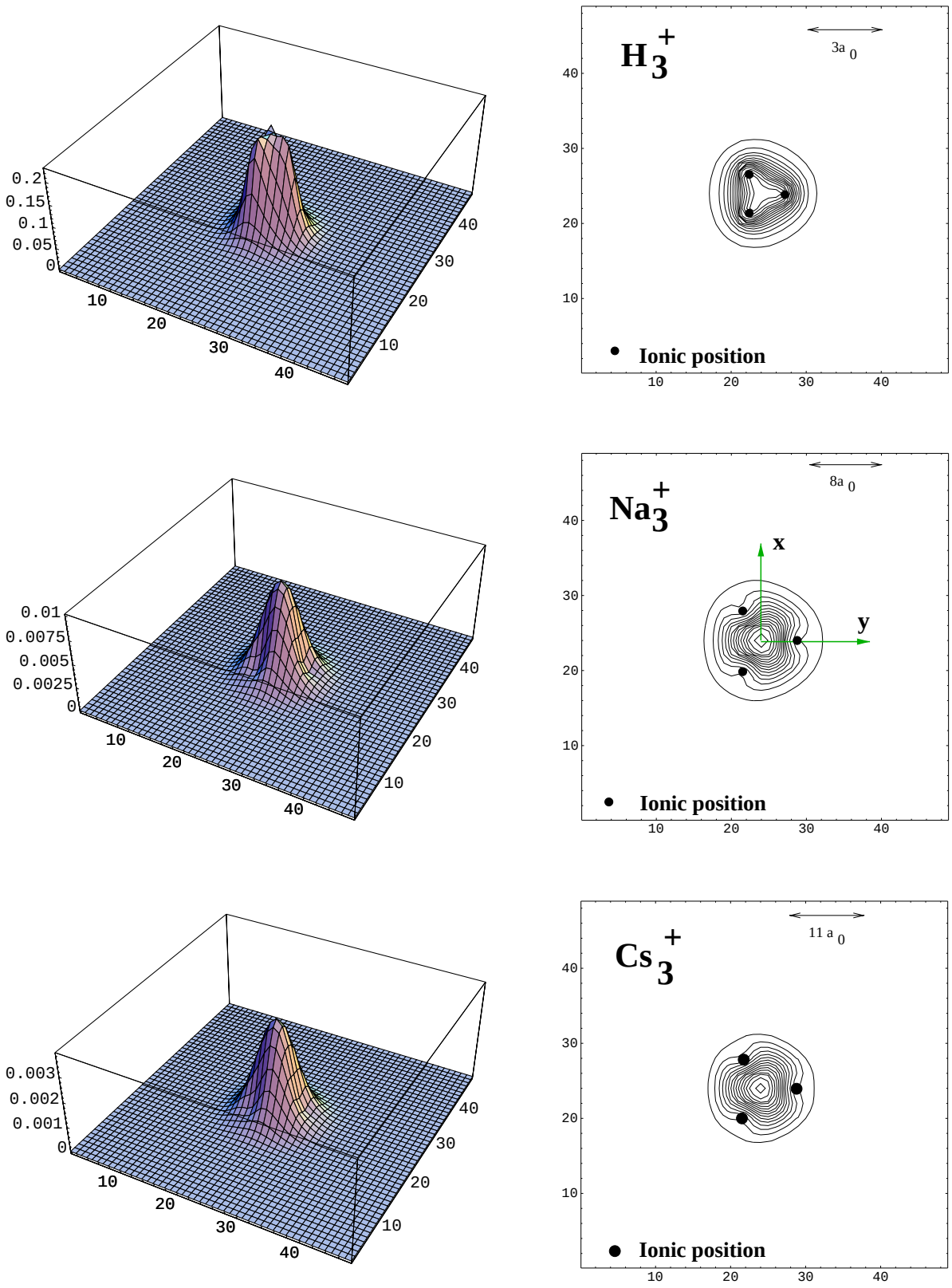

Fig. 1. Electronic density distributions for the ground states of H_3^+, Na_3^+, and Cs_3^+. The left panels visualise the densities in the x–y-plane as 3D plots. The right panels do the same in terms of equidensity contour plots. They also indicate the position of the ions by a dot. The plotting boxes are always chosen to represent the full numerical grid. The coordinates of the boxes are given in units of mesh spacings Δ, as indicated on each panel of the right column.

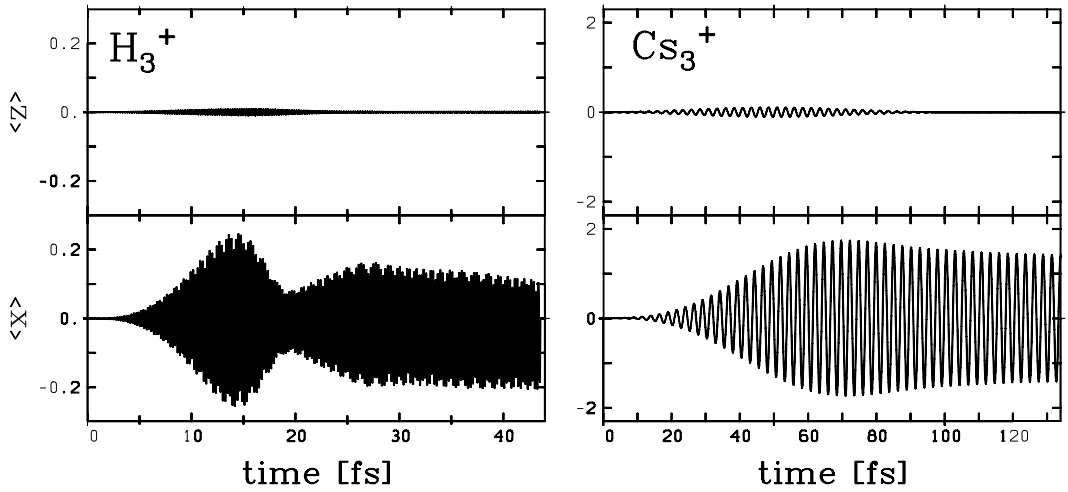

Fig. 2. Time evolution of dipole moment along x- and z-directions. Left: for the H_3^+ cluster. Right: for the Cs_3^+ cluster. Both systems are excited in their linear regime. The laser parameters used for the left figure are $I = 10^{11}$ W cm^{-2} with a pulse duration $T_{\rm pulse} = 30$ fs and laser frequency 18.1 eV, whereas for the right one $I = 10^9$ W cm^{-2}, $T_{\rm pulse} = 100$ fs and laser frequency 1.66 eV.

the fact that the more tightly bound electrons in H_3^+ need stronger fields to react. One may also wonder why the resonant response for H_3^+ has a waistline (beyond 20 fs). This comes from the fact that the laser pulse was slightly detuned (by 0.1 eV) from the very sharp resonance frequency of the x-mode. There is thus a beating between the laser frequency and the resonance. On the contrary, in the case of Cs, the wider (more "metallic") resonance at 1.6 eV in x-direction (Tab. 4) is directly attached by the laser during the pulse itself and the oscillatory pattern along x continues unaffected, at the resonance frequency, once the laser has been switched off. The case thus demonstrates that the time evolution of the response is a very sensitive probe.

Another *a priori* curious feature is the small drift of the x-dipole signal at large times seen only for H_3^+. This effect is due to the motion of the ionic background, which, mind it, sets on much more quickly for hydrogen than for cesium (see vibration periods in Tab. 3). We have to remind that these calculations have been done with full TDLDA-MD allowing the ions to take part into the motion. But the mass of the proton is much smaller than the mass of the Cs ion. And thus it starts to move at a much shorter time scale. We can estimate that scale: we know from Na clusters that ionic motion makes effects on the electronic response at about 50–100 fs [6,25]. The mass ratio to H is 1/23 and the times scale with $\sqrt{1/23} \approx 1/5$. We thus have to expect ionic effects for H clusters already at around 10–20 fs. The drift for the case of H_3^+ is hence very well in time.

An explicit check of the time scale at which ions couple to the motion is given by the difference in response between TDLDA (without ionic motion) and TDLDA-MD. One example at higher intensity is shown in Figure 3 in the case of H_2 (see also Sect. 3.2.2). The signals for ionisation obviously deviate from each other from 10 fs on. This provides a direct proof that ionic motion comes into play very early for the case of hydrogen clusters. It is also interesting to note the sizable difference in the asymptotic values of ionisation attained by the irradiated H_2. Under the same laser conditions ionic motion leads, in this case, to a doubling of final ionisation. Of course, the actual difference depends on the laser parameters, but, as we shall see below, the effect is always large.

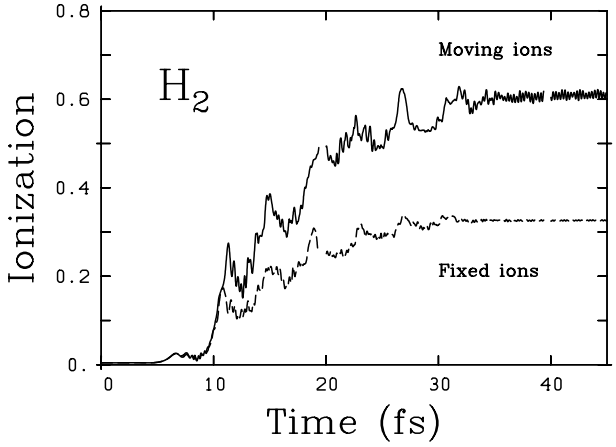

Fig. 3. Ionisation as function of time for H_2. A case with and without ionic motion is compared. Laser duration was $T_{\rm pulse} = 40$ fs, frequency $\omega = 0.5$ eV and intensity $I = 4 \times 10^{14}$ W cm^{-2}, polarisation along H_2-axis.

3.2.2 Non linear dynamics

The case of non linear excitations, as attained by more intense laser pulses, is illustrated in Figure 4 which shows a typical example of response of Cs_3^+ in the non-linear regime. The uppermost panel gives a protocol of ionisation in the course of time. In that case we loose finally in the average about 0.6 electrons. (Mind that we discuss

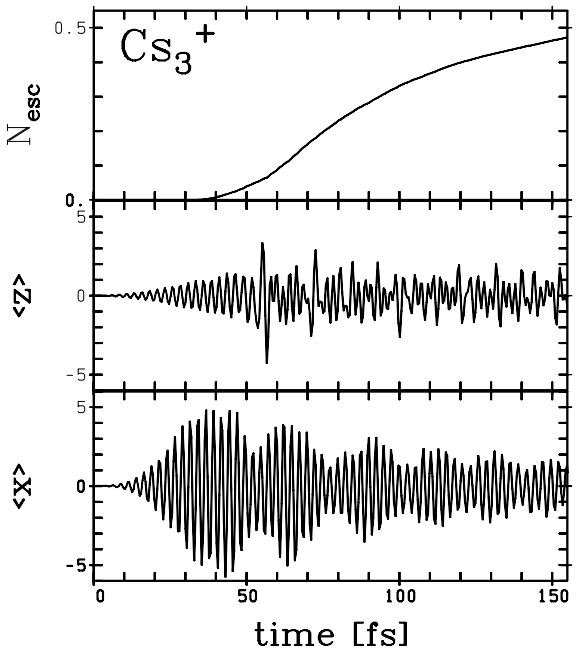

Fig. 4. Time evolution of ionisation (upper panel) and of dipole momentum along x- and z-direction for the Cs_3^+ molecule excited in the non-linear regime by a laser with $I = 10^{11}$ W cm^{-2} and $T_{\rm pulse} = 100$ fs and frequency 1.66 eV.

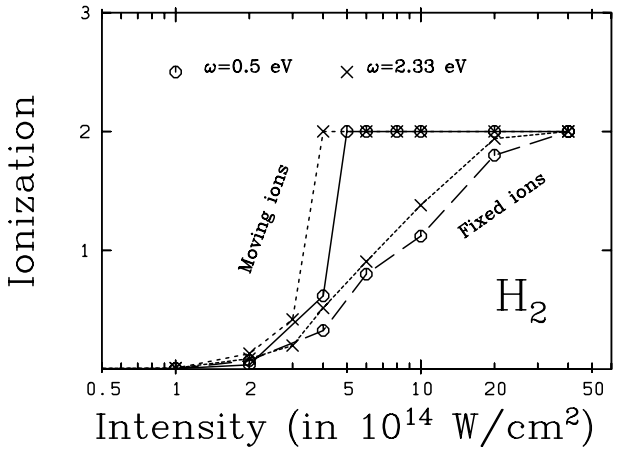

Fig. 5. Final ionisation as function of laser intensity for the case of H_2. Two different laser frequencies had been used as indicated. Pulse length was $T_{\rm pulse} = 40$ fs, polarisation along H_2-axis. We compare propagation with ionic MD and with frozen ions.

here an average value of ionisation and not detailed ionisation probabilities, as *e.g.* in [24].) Such strong ionisation is always a typical indicator that we have entered the non-linear regime. (We had practically no ionisation at all for the above two test cases in the linear regime.) The dipole signals show some significant differences as compared to the linear case. The x-mode starts out similar as before. But note that the signal experiences a much stronger damping in the course of time. That is mainly due to ionisation and also to enhanced Landau damping at this more energetic excitation. The z-mode is significantly more strongly responding than in the linear case. There is more cross talk due to the larger fluctuations of the electron cloud and the increased width of the mode gives larger overlap with the laser frequency. Note particularly the sort of chaotic pattern developing in the z signal which is again related to the strong density fluctuations. Note, furthermore, that the large mass of the Cs ions prevents any visible effect due to the ionic motion in the case of Cs_3^+, on the 150 fs time scale we are considering here.

As we have seen above, the low proton mass makes ionic motion much more important for hydrogen clusters, even for fairly short fs laser pulses. Figure 5 presents a systematic survey of the ionic effects on ionisation in the case of H_2. We look at the final ionisation as a function of laser intensity for a rather short pulse with $T_{\rm pulse} = 40$ fs. Two different frequencies are considered. One far below any excitation state and the other a bit closer to the first excitation. Still, remind that the dipole eigenfrequencies lie well above both laser frequencies, namely in the 18–20 eV range. Both frequencies yield very similar pattern (for the high intensities visible in that plot). But there is a significant difference between the case with and without ionic motion. The transition to full ionisation proceeds much more rapidly if ionic motion is active. The effect is due to the Coulomb expansion induced by ionisation. The molecular distance grows and subsequently the ionisation threshold shrinks. This enhances ionisation in the course of time and the more so the larger the intensity. Consequently, ionisation raises more rapidly when ionic motion is allowed. This effect exists, of course, also for other materials. But it requires correspondingly longer laser pulses to come into such a sizable regime of enhanced ionisation.

4 Conclusions

In this paper we have demonstrated the capability of TDLDA-MD to describe cluster dynamics for various materials in the linear as well as in the non linear domain. We have shown that this approach provides a relevant description of basic atomic and molecular properties including optical response. Response to intense lasers under varying conditions has shown differences which come from different electronic binding properties (covalent *versus* metallic). The small mass of hydrogen furthermore leads to a particularly quick coupling to ionic degrees of freedom. A correct (dynamical) treatment of ionic degrees of freedom is thus crucial in the case of hydrogen clusters. As one example, we find that ionisation in H_2 is strongly enhanced by the actual ionic expansion, even for rather short laser pulses. Extension of these calculations to more massive hydrogen clusters is underway.

This work has been supported by the French-German exchange program PROCOPE, contract number 99074, and by the Institut Universitaire de France.

References

1. U. Kreibig, M. Vollmer, *Optical properties of metal clusters* (Springer Series in Materials Science, 1993), Vol. 25.
2. Faisal, *Theory of Multiphoton Processes* (Plenum Press, New York, 1987)
3. J. Zweiback *et al.*, Phys. Rev. Lett. **84**, 2634 (2000).
4. L. Köller, M. Schumacher, J. Köhn, S. Teuber, J. Tiggesbäumker, K.-H. Meiwes-Broer, Phys. Rev. Lett. **82**, 3783 (1999).
5. *NATO ASI Series B*, edited by E.K.U. Gross, R.M. Dreizler (Plenum Press, New York, 1995), Vol. 337.
6. F. Calvayrac, P.-G. Reinhard, E. Suraud, C. Ullrich, Phys. Rep. **337**, 493 (2000).
7. E. Suraud, P.-G. Reinhard, Phys. Rev. Lett. **85**, 2296 (2000).
8. F. Calvayrac, P.-G. Reinhard, E. Suraud, J. Phys. B **31**, 5023 (1998).
9. L.B. DaSilva *et al.*, Phys. Rev. Lett. **78**, 483 (1997).
10. T. Ditmire *et al.*, Nature **398**, 489 (1999).
11. J.P. Perdew, Y. Wang, Phys. Rev. B **45**, 13244 (1992).
12. S. Kümmel *et al.*, Eur. J. Phys. D **9**, 149 (1999).
13. S. Kümmel (private communication).
14. J.P. Perdew, A. Zunger, Phys. Rev. B **23**, 5048 (1981).
15. V. Blum, G. Lauritsch, J.A. Maruhn, P.-G. Reinhard, J. Comp. Phys. **100**, 364 (1992).
16. F. Calvayrac, Ann. Phys. Fr. **23**(3), 1 (1998).
17. F. Calvayrac, P.-G. Reinhard, E. Suraud, Phys. Rev. B **52**, R17056 (1995).
18. K. Yabana, G.F. Bertsch, Phys. Rev. B **54**, 4484 (1996).
19. F. Calvayrac, P.-G. Reinhard, E. Suraud, Ann. Phys. (NY) **255**, 125 (1997).
20. V. Bonacic-Koutecky, J. Pittner, C. Fuchs, P. Fantucci, M.F. Guest, J. Koutecky, J. Chem. Phys. **104**, 1427 (1996).
21. S. Kuemmel, J. Akola, M. Manninen, Phys. Rev. Lett. **84**, 3827 (2000).
22. M. Schmidt, H. Haberland, Eur. Phys. J. D **6**, 109 (1999).
23. P.-G. Reinhard, E. Suraud, Eur. Phys. J. D **3**, 175 (1998).
24. C.A. Ullrich, P.-G. Reinhard, E. Suraud, J. Phys. B **30**, 5043 (1997).
25. P.-G. Reinhard, F. Calvayrac, C. Kohl, S. Kümmel, E. Suraud, C.A. Ullrich, M. Brack, Eur. Phys. J. D **9**, 111 (1999).
26. `http://webbook.nist.gov/chemistry/`